COBEM UBERLÂNDIA 2019

ABCM Associação Brasileira de Engenharia e Ciências Mecânicas

25th ABCM International Congress of Mechanical Engineering
October 20-25, 2019, Uberlândia, MG, Brazil

COB-2019-0715
COUPLED STRETCHING-BENDING ANALYSIS OF ASSEMBLED THIN LAMINATED PLATE STRUCTURES VIA BOUNDARY ELEMENTS

Caio César Rocha Ramos
Carlos Henrique Daros
Department of Computational Mechanics, Faculty of Mechanical Engineering, State University of Campinas, 200 Mendeleyev Street, 13083-860, Campinas, SP, Brazil.
caioramos85@gmail.com, chdaros@fem.unicamp.br

Abstract. *Recently, a boundary element formulation for the coupled stretching-bending analysis of thin laminated plates has been developed. The related boundary integral equations were obtained with the aid of the Betti-Rayleigh reciprocal theorem and the fundamental solutions were derived through the use of a Stroh-like complex variable formalism. Here, this formulation is extended in order to cover problems of assembled thin laminated plate structures by means of the subregions technique. Following this approach, each plate is considered separately and then joined together by imposing equilibrium conditions and displacement compatibility along interface edges. Furthermore, remaining domain integrals present in the original formulation, related to distributed loads, are transformed into boundary integrals using the radial integration method. Some examples are presented and the numerical results are compared with those provided by a finite element software, certifying the reliability and accuracy of the present formulation.*

Keywords: *Boundary Element Method, Coupled stretching-bending analysis, Composite laminates, Plates.*

1. INTRODUCTION

When the laminae stacking sequence is non-symmetrical with respect to the midplane of the plate, the coupling of in-plane and plate bending problems unavoidably arises. Thus, the coupled stretching-bending must be taken into account in order to establish a formulation able to cover all the possibility of symmetric or unsymmetric thin laminated plates.

Hwu (2003) presented a complex variable Stroh-like formalism for the coupled stretching-bending analysis of general laminated plates and, by using this formalism and the Betti-Rayleigh reciprocal theorem, Hwu (2010) derived the fundamental solutions and boundary integral equations required for boundary element method (BEM). Later, Hwu (2012) stated the very first boundary element formulation, which assumed linear variation for all functions except the deflection which was described as a third-order polynomial due to the requirement of continuous slope. Hwu and Chang (2015a) studied four different approaches to deal with corners. Lastly, Hwu and Chang (2015b) provided analytical solutions for all the singular integrals and Chang and Hwu (2016) got complete solutions at and near the boundary nodes.

The coupled stretching-bending analysis of assembled thin laminated plate structures via boundary elements, to the best of the authors' knowledge, is presented here for the first time. Moreover, domain integrals related to distributed loads are transformed into boundary integrals through radial integration method (Gao, 2002), recovering the pure boundary character of the BEM and, hence, its associated advantages.

2. BOUNDARY ELEMENT FORMULATION

The boundary integral equations for the coupled stretching-bending analysis of thin laminated plates (Fig. 1), derived in Hwu (2010) and modified in Hwu (2012), can be written as

$$C_{ip}(\boldsymbol{\xi})u_p(\boldsymbol{\xi}) + \int_\Gamma^* t^*_{ij}(\boldsymbol{\xi},\mathbf{x})\breve{u}_j(\mathbf{x})d\Gamma(\mathbf{x}) + \sum_{k=1}^{N_c^*} t^*_{ic}(\boldsymbol{\xi},\mathbf{x}_k)\breve{u}_3(\mathbf{x}_k) = \int_\Gamma u^*_{ij}(\boldsymbol{\xi},\mathbf{x})t_j(\mathbf{x})d\Gamma(\mathbf{x}) + \int_A u^*_{ij}(\boldsymbol{\xi},\mathbf{x})q_j(\mathbf{x})dA(\mathbf{x}) + \sum_{k=1}^{N_c^*} u^*_{i3}(\boldsymbol{\xi},\mathbf{x}_k)t_c(\mathbf{x}_k)$$

$$i,j = 1,2,3,4, \quad p = 1,2,3,4,5, \tag{1}$$

where

$$\breve{u}_i(\mathbf{x}) = u_i(\mathbf{x}), \quad i = 1,2,4, \quad \breve{u}_3(\mathbf{x}) = u_3(\mathbf{x}) - u_3(\boldsymbol{\xi}), \tag{2}$$

and

$$
\begin{aligned}
&u_1 = u_0, \quad u_2 = v_0, \quad u_3 = w, \quad u_4 = \beta_n, \quad u_5 = \beta_s, \\
&t_1 = T_x, \quad t_2 = T_y, \quad t_3 = V_n, \quad t_4 = M_n, \quad t_c = M_{ns}^{+} - M_{ns}^{-}, \\
&q_1 = q_x, \quad q_2 = q_y, \quad q_3 = q, \quad q_4 = m_n.
\end{aligned} \tag{3}
$$

In the above equations, Γ and A are the boundary and surface region of the plate; $\int^*$ denotes an integral taken in the sense of Cauchy principal value; $C_{ip}(\boldsymbol{\xi})$, $i = 1,2,3,4$, $p = 1,2,3,4,5$, are the free term coefficients; u_0, v_0 and w are the midplane displacements in x, y and z directions; $\beta_n = -\partial w/\partial n$ and $\beta_s = -\partial w/\partial s$ are the negative slopes of deflection in normal ($\mathbf{n}$) and tangential ($\mathbf{s}$) directions; T_x and T_y are the x and y components of surface traction; V_n and M_n are the effective transverse shear force and bending moment on the surface with normal direction $\mathbf{n}$; t_c is the corner force related to the twisting moments M_{ns} ahead $(+)$ and behind $(-)$ of the corner; q_x, q_y, q and m_n represent the distributed loads in x, y, z directions and moment in n direction, which is the direction of the applied distributed moment and should not be confused with the boundary normal. $u_{ij}^*(\boldsymbol{\xi},\mathbf{x})$, $t_{ij}^*(\boldsymbol{\xi},\mathbf{x})$ and $t_{ic}^*(\boldsymbol{\xi},\mathbf{x})$, $i = 1,2,3$, $j = 1,2,3,4$, are the fundamental solutions which represent, respectively, u_j, t_j and t_c at a field point $\mathbf{x}$ corresponding to a unit point force acting in the x_i direction applied at the source point $\boldsymbol{\xi}$, whereas $u_{4j}^*(\boldsymbol{\xi},\mathbf{x})$, $t_{4j}^*(\boldsymbol{\xi},\mathbf{x})$, $t_{4c}^*(\boldsymbol{\xi},\mathbf{x})$, $j = 1,2,3,4$, represent u_j, t_j and t_c at $\mathbf{x}$ corresponding to a unit point moment acting on the surface with normal $\mathbf{n}$ applied at $\boldsymbol{\xi}$. N_c is the number of corners and N_c^* denotes that when the source point is a corner, the set of points $\mathbf{x}_k$ should include all corners except the source point itself. Expressions for fundamental solutions and free term coefficients can be found in Hwu (2010) and Hwu (2012).

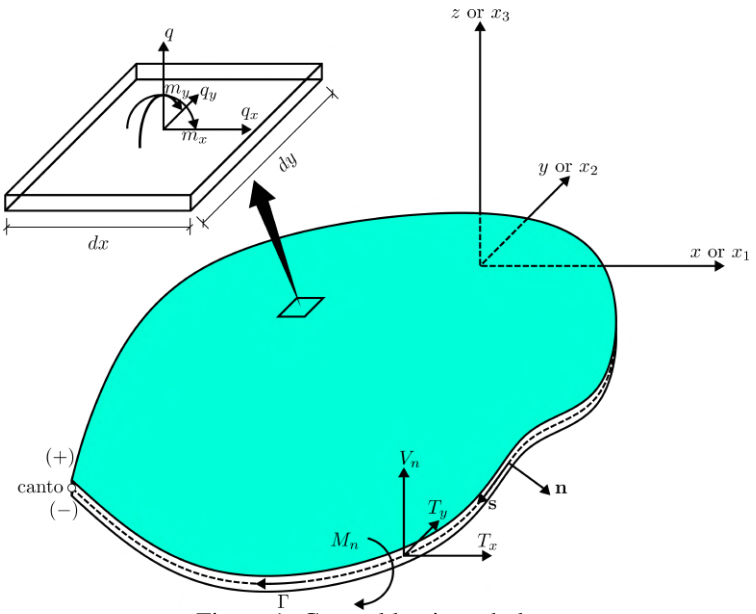

Figure 1: General laminated plate

The system of linear algebraic equations obtained via BEM, discretizing the boundary Γ into M segments with N nodes, can be written as (Hwu, 2012; Hwu and Chang, 2015a)

$$
\begin{aligned}
&\sum_{j=1}^{N} \{\mathbf{Y}_{ij}\mathbf{u}_j - \mathbf{G}_{ij}\mathbf{t}_j\} + \sum_{k=1}^{N_c^*} \left\{\mathbf{p}_{ik}^* w_c^{(k)} - \mathbf{w}_{ik}^* t_c^{(k)}\right\} = \mathbf{q}_i^*, \quad i = 1,2,\ldots,N, \\
&\sum_{j=1}^{N} \{\mathbf{y}_{ij}\mathbf{u}_j - \mathbf{g}_{ij}\mathbf{t}_j\} + \sum_{k=1}^{N_c^*} \left\{p_{ik}^{*(3)} w_c^{(k)} - w_{ik}^{*(3)} t_c^{(k)}\right\} = q_i^{*(3)}, \quad i = 1,2,\ldots,N_c,
\end{aligned} \tag{4}
$$

where $\mathbf{Y}_{ij}$ and $\mathbf{G}_{ij}$ are 4×4 matrices of influence coefficients; $\mathbf{u}_j$ and $\mathbf{t}_j$ are vectors of nodal displacements and nodal tractions; $\mathbf{p}_{ik}^*$ and $\mathbf{w}_{ik}^*$ are 4×1 vectors related to the fundamental solutions of corner forces and deflection; w_c is the corner deflection; $\mathbf{q}_i^*$ is a vector related to the distributed loads and moments; $\mathbf{y}_{ij}$ and $\mathbf{g}_{ij}$ are two 1×4 matrices extracted from the third row of $\mathbf{Y}_{ij}$ and $\mathbf{G}_{ij}$, respectively; whereas $p_{ik}^{*(3)}$, $w_{ik}^{*(3)}$ and $q_i^{*(3)}$ are, respectively, the third components of the vectors $\mathbf{p}_{ik}^*$, $\mathbf{w}_{ik}^*$ and $\mathbf{q}_i^*$. Thus, Eq. (4) produces a $(4N + N_c) \times (4N + N_c)$ system of equations. Detailed expressions for influence coefficients can be found in Hwu (2012) and Hwu and Chang (2015a). The basic variables of the boundary element formulation are the nodal displacements and tractions, arranged into vectors $\mathbf{u}_j$ and $\mathbf{t}_j$, respectively. Also, each corner add two variables to the formulation: corner force t_c and deflection w_c. Thus, the boundary element formulation requires that either u_i or t_i at each node and either w_c or t_c at each corner are prescribed.

The treatment of corners suggested in Hwu and Chang (2015a) locates three nodes on the same position of the corner, as shown in Fig. 2. Two nodes ($\boldsymbol{\xi}^+$ and $\boldsymbol{\xi}^-$) are selected to represent the two sides of a corner and, hence, have different normal directions. Consequently, their values of β_n, T_x, T_y, V_n and M_n are different. For each one of these nodes, four equations are written. A third node ($\boldsymbol{\xi}$) is placed and its associated variables are the corner force t_c and deflection w_c. For this node, only one equation is written. Through this approach, a set of nine equations are written for each corner, with five being always independent each other since two nodes have different normal direction and the other four, which correspond to the first, second and third equations written for $\boldsymbol{\xi}^+$ and the single equation for $\boldsymbol{\xi}$, can be respectively replaced by

$$\begin{aligned}
&C_{i1}\left(u^- - u^+\right) + C_{i2}\left(v_0^- - v_0^+\right) + C_{i3}\left(w^- - w^+\right) = 0, \quad i = 1, 2,\\
&w^- - w^+ = 0,\\
&w^- - w_c = 0.
\end{aligned} \tag{5}$$

The displacement components denoted with superscripts $+$ and $-$ represent values immediately ahead of and behind the corner, respectively, whereas w_c stands for corner deflection associated to the third node $\boldsymbol{\xi}$.

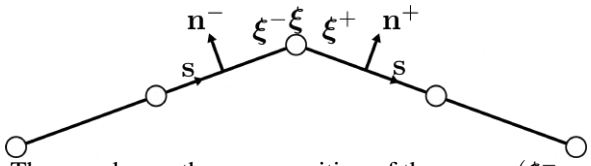

Figure 2: Three nodes on the same position of the corner ($\boldsymbol{\xi}^- = \boldsymbol{\xi}^+ = \boldsymbol{\xi}$)

Depending on the boundary conditions applied, none, one, two or four equations in Eq. (5) may be automatically satisfied. For instance, the boundary conditions associated to a corner connecting two clamped edges consist of the following information: $w^- = w^+ = w_c = u_0^- = u_0^+ = v_0^- = v_0^+ = 0$, which leads all equations in Eq. (5) to $0 = 0$. Thus, this approach requires four auxiliary equations to make up for the equation dependency raised by using coincident nodes. These auxiliary equations were derived in Hwu and Chang (2015a) considering the symmetry of stress tensor and using the laminate constitutive relations.

The above formulation has provided accurate solutions for symmetric, unsymmetric and anti-symmetric laminated plates with or without holes (Hwu, 2012; Hwu and Chang, 2015a,b; Chang and Hwu, 2016). However, dealing with assembled plates, some problems appear at the corners. For example, assuming a plate arbitrarily defined in a three-dimensional space (Fig. 3), the corner deflection w_c, in the direction transverse to the plate, must be decomposed into a linear combination of three components in global directions, but the third node $\boldsymbol{\xi}$ has only one degree of freedom and one equation. To avoid dealing with these difficulties, the corner reactions were neglected. Through this way, Eq. (4) can be modified as

$$\begin{aligned}
&\sum_{j=1}^{N}\left\{\mathbf{Y}_{ij}\mathbf{u}_j - \mathbf{G}_{ij}\mathbf{t}_j\right\} + \sum_{k=1}^{N_c^*}\left\{\mathbf{p}_{ik}^* w_c^{(k)}\right\} = \mathbf{q}_i^*, \quad i = 1, 2, \ldots, N,\\
&\sum_{j=1}^{N}\left\{\mathbf{y}_{ij}\mathbf{u}_j - \mathbf{g}_{ij}\mathbf{t}_j\right\} + \sum_{k=1}^{N_c^*}\left\{p_{ik}^{*(3)} w_c^{(k)}\right\} = q_i^{*(3)}, \quad i = 1, 2, \ldots, N_c.
\end{aligned} \tag{6}$$

As previously discussed, the equation written for the third node can be replaced by $w^- - w_c = 0$. Thus, the set of N_c equations in Eq. (6) can be expressed as

$$w^{-(k)} - w_c^{(k)} = 0, \quad i = 1, 2, \ldots, N_c. \tag{7}$$

By simply applying the N_c equations in Eq. (7) directly in the N equations written for the other nodes, i.e assuming $w_c^{(k)} = w^{-(k)}$, Eq. (6) can be reduced to a $4N \times 4N$ system of equations, presented below

$$\sum_{j=1}^{N}\left\{\widetilde{\mathbf{Y}}_{ij}\mathbf{u}_j - \mathbf{G}_{ij}\mathbf{t}_j\right\} = \mathbf{q}_i^*, \quad i = 1, 2, \ldots, N, \tag{8}$$

where

$$\{\widetilde{Y}_{mn}\}_{ij} = \{Y_{mn}\}_{ij}, \quad m = 1, 2, 3, 4, \quad n = 1, 2, 4, \tag{9}$$

and

$$\{\widetilde{Y}_{m3}\}_{ij} = \begin{cases} \{Y_{m3}\}_{ij}, & \text{if } j \text{ is a regular node or a corner node } (+), \quad m = 1, 2, 3, 4,\\ \{Y_{m3}\}_{ij} + \{p_m^*\}_{ik}, & \text{if } j \text{ is a corner node } (-), \quad m = 1, 2, 3, 4. \end{cases} \tag{10}$$

In the above, the subscript k is the number corresponding to the corner coincident with j when it is a corner node $(-)$. As both variables related to the third node vanished from the formulation, only two nodes are required for each corner.

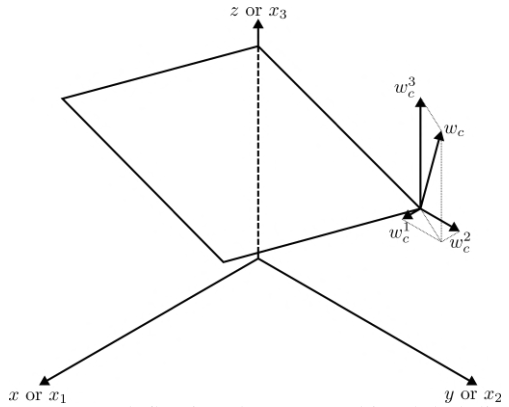

Figure 3: Corner deflection decomposed in global directions

3. BOUNDARY INTEGRAL FORM FOR COEFFICIENTS RELATED TO DISTRIBUTED LOADS

The domain integral along the surface region of the plate present in the boundary integral equations (Eq. (1)) for the coupled stretching-bending analysis can be expressed as

$$q_i^*(\boldsymbol{\xi}) = \int_A u_{ij}^*(\boldsymbol{\xi}, \mathbf{x}) q_j(\mathbf{x}) dA(\mathbf{x}). \tag{11}$$

The fundamental solutions, in terms of the polar coordinate (r, φ) with origin located at the source point $\boldsymbol{\xi}$, can be written as (Hwu, 2012)

$$\begin{aligned}
u_{ij}^*(\boldsymbol{\xi}, \mathbf{x}) &= u_{ij}(\varphi) \ln r + u_{ij}^0(\varphi), \quad i, j = 1, 2, 4, \\
u_{3j}^*(\boldsymbol{\xi}, \mathbf{x}) &= u_{3j}(\varphi) r (\ln r - 1) + r u_{3j}^0(\varphi), \quad j = 1, 2, 4, \\
u_{i3}^*(\boldsymbol{\xi}, \mathbf{x}) &= u_{i3}(\varphi) r (\ln r - 1) + r u_{i3}^0(\varphi), \quad i = 1, 2, 4, \\
u_{33}^*(\boldsymbol{\xi}, \mathbf{x}) &= u_{33}(\varphi) r^2 (2 \ln r - 3) + r^2 u_{33}^0(\varphi).
\end{aligned} \tag{12}$$

Detailed expressions for the complex functions $u_{ij}(\varphi)$ and $u_{ij}^0(\varphi)$ are presented in Hwu (2012).

The integrand in Eq. (11) contains the term $q_j(\mathbf{x})$ which represents the surface load evaluated at the internal field point $\mathbf{x}$. In the integral over the domain the source point is fixed whereas the field point assumes the position of all points in A. In order to distinguish these points from field points located at the boundary, we can replace $q_j(\mathbf{x})$ and $u_{ij}^*(\boldsymbol{\xi}, \mathbf{x})$ by $q_j(x)$ and $u_{ij}^*(\boldsymbol{\xi}, x)$, with x representing the Cartesian coordinates for every point of the surface region (x_1, x_2).

Consider a rectangular plate under a non-uniformly distributed load $q_j(x)$ as represented in Fig. 4. Let P_i^j denote $q_j(x)$ evaluated at the corner i. Considering the coordinate system located at the center of the plate, $q_j(x)$ can be interpolated from P_i^j values as follows

$$\begin{aligned}
q_j(x) = \left(\frac{P_3^j - P_2^j + P_4^j - P_1^j}{2l_1} \right) x_1 + \left(\frac{P_2^j - P_1^j + P_3^j - P_4^j}{2l_2} \right) x_2 \\
+ \left(\frac{P_1^j + P_2^j + P_3^j + P_4^j}{4} \right) + \left(\frac{P_1^j - P_2^j + P_3^j - P_4^j}{l_1 l_2} \right) x_1 x_2.
\end{aligned} \tag{13}$$

In this work, general loads matching the same form as Eq. (13) are taken into consideration, i.e.

$$q_j(x) = a_j x_1 + b_j x_2 + c_j + d_j x_1 x_2, \tag{14}$$

where a_j, b_j, c_j and d_j are known constants.

According to the radial integration method, described in Gao (2002), for a general two-dimensional function $f(x)$, its domain integral can be transformed into the following boundary integral

$$\int_A f(x) dA = \int_\Gamma \frac{1}{r} \frac{\partial r}{\partial n} F(Q) d\Gamma(Q), \quad \text{where,} \quad F(Q) = \int_0^{r(Q)} f(x) r dr. \tag{15}$$

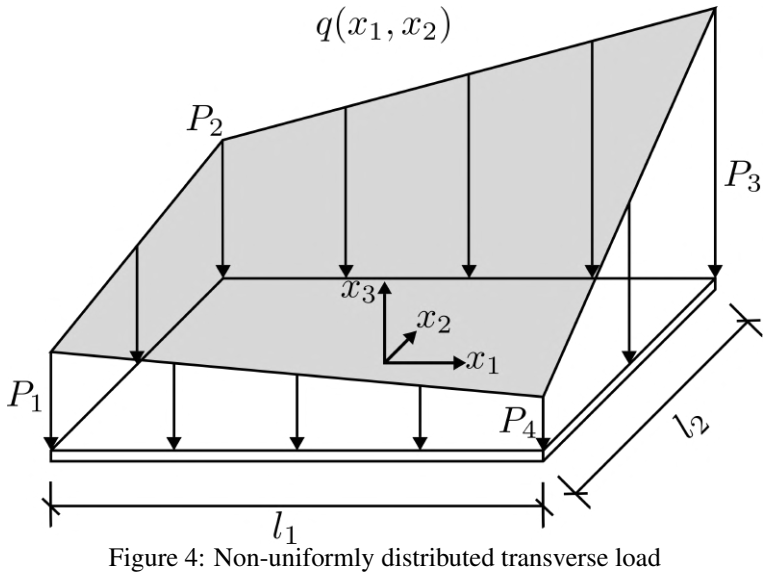

Figure 4: Non-uniformly distributed transverse load

The symbol Q indicates that the field point for the boundary integral is on the boundary Γ. Substituting the integrand of Eq. (11) into the radial integral in Eq. (15) and assuming $q_j(x)$ as in Eq. (14), we get

$$F_i(\boldsymbol{\xi}, \mathbf{x}) = \int_0^{r(\mathbf{x})} u^*_{ij}(\boldsymbol{\xi}, x) q_j(x) r dr = \int_0^{r(\mathbf{x})} u^*_{ij}(\boldsymbol{\xi}, x) \left(a_j x_1 + b_j x_2 + c_j + d_j x_1 x_2\right) r dr, \tag{16}$$

where $\mathbf{x}$ plays the same role of Q in Eq. (15), denoting a field point on the boundary. To evaluate the above radial integral, $u^*_{ij}(\boldsymbol{\xi}, x)$, x_1 and x_2 need to be expressed in terms of the distance r. This can be done by using Eq. (12) and the following expressions

$$x_i = x_i^p + r_{,i} r, \quad r_{,i} = \frac{\partial r}{\partial x_i} = \frac{r_i}{r}, \quad r_i = x_i - x_i^p, \tag{17}$$

in which x_i^p represents the Cartesian coordinates at the source point.

Substituting Eq. (12) and Eq. (17) into Eq. (16) and performing the resulting integrals, the following results are obtained

$$F_i(\boldsymbol{\xi}, \mathbf{x}) = r \left[F^1_{ij}(\boldsymbol{\xi}, \mathbf{x}) q^1_j(\boldsymbol{\xi}, \mathbf{x}) + F^2_{ij}(\boldsymbol{\xi}, \mathbf{x}) q^2_j(\boldsymbol{\xi}, \mathbf{x}) + F^3_{ij}(\boldsymbol{\xi}, \mathbf{x}) q^3_j(\boldsymbol{\xi}, \mathbf{x})\right], \tag{18}$$

where

$$\begin{aligned}
&F^1_{ij}(\boldsymbol{\xi}, \mathbf{x}) = r \left[\frac{u^0_{ij}(\varphi)}{2} + u_{ij}(\varphi)\left(\frac{1}{2}\ln r - \frac{1}{4}\right)\right], \qquad F^2_{ij}(\boldsymbol{\xi}, \mathbf{x}) = r^2 \left[\frac{u^0_{ij}(\varphi)}{3} + u_{ij}(\varphi)\left(\frac{1}{3}\ln r - \frac{1}{9}\right)\right], \\
&F^3_{ij}(\boldsymbol{\xi}, \mathbf{x}) = r^3 \left[\frac{u^0_{ij}(\varphi)}{4} + u_{ij}(\varphi)\left(\frac{1}{4}\ln r - \frac{1}{16}\right)\right], \quad i, j = 1, 2, 4, \\
&F^1_{3j}(\boldsymbol{\xi}, \mathbf{x}) = r^2 \left[\frac{u^0_{3j}(\varphi)}{3} + u_{3j}(\varphi)\left(\frac{1}{3}\ln r - \frac{4}{9}\right)\right], \qquad F^2_{3j}(\boldsymbol{\xi}, \mathbf{x}) = r^3 \left[\frac{u^0_{3j}(\varphi)}{4} + u_{3j}(\varphi)\left(\frac{1}{4}\ln r - \frac{5}{16}\right)\right], \\
&F^3_{3j}(\boldsymbol{\xi}, \mathbf{x}) = r^4 \left[\frac{u^0_{3j}(\varphi)}{5} + u_{3j}(\varphi)\left(\frac{1}{5}\ln r - \frac{6}{25}\right)\right], \quad j = 1, 2, 4, \\
&F^1_{i3}(\boldsymbol{\xi}, \mathbf{x}) = r^2 \left[\frac{u^0_{i3}(\varphi)}{3} + u_{i3}(\varphi)\left(\frac{1}{3}\ln r - \frac{4}{9}\right)\right], \qquad F^2_{i3}(\boldsymbol{\xi}, \mathbf{x}) = r^3 \left[\frac{u^0_{i3}(\varphi)}{4} + u_{i3}(\varphi)\left(\frac{1}{4}\ln r - \frac{5}{16}\right)\right], \\
&F^3_{i3}(\boldsymbol{\xi}, \mathbf{x}) = r^4 \left[\frac{u^0_{i3}(\varphi)}{5} + u_{i3}(\varphi)\left(\frac{1}{5}\ln r - \frac{6}{25}\right)\right], \quad i = 1, 2, 4, \\
&F^1_{33}(\boldsymbol{\xi}, \mathbf{x}) = r^3 \left[\frac{u^0_{33}(\varphi)}{4} + u_{33}(\varphi)\left(\frac{1}{2}\ln r - \frac{7}{8}\right)\right], \qquad F^2_{33}(\boldsymbol{\xi}, \mathbf{x}) = r^4 \left[\frac{u^0_{33}(\varphi)}{5} + u_{33}(\varphi)\left(\frac{2}{5}\ln r - \frac{17}{25}\right)\right], \\
&F^3_{33}(\boldsymbol{\xi}, \mathbf{x}) = r^5 \left[\frac{u^0_{33}(\varphi)}{6} + u_{33}(\varphi)\left(\frac{1}{3}\ln r - \frac{10}{18}\right)\right],
\end{aligned} \tag{19}$$

and

$$q_j^1(\boldsymbol{\xi},\mathbf{x}) = a_j x_1^p + b_j x_2^p + + c_j + d_j x_1^p x_2^p, \quad q_j^2(\boldsymbol{\xi},\mathbf{x}) = a_j r_{,1} + b_j r_{,2} + d_j r_{,1} x_2^p + d_j r_{,2} x_1^p, \quad q_j^3(\boldsymbol{\xi},\mathbf{x}) = d_j r_{,1} r_{,2}. \tag{20}$$

Substituting Eq. (18) into Eq. (15), we get the boundary integral form for $q_i^*(\boldsymbol{\xi})$, which can be expressed as

$$q_i^*(\boldsymbol{\xi}) = \int_A u_{ij}^*(\boldsymbol{\xi},\mathbf{x}) q_j(\mathbf{x}) dA(\mathbf{x}) = \int_\Gamma \frac{\partial r}{\partial n} \left[F_{ij}^1(\boldsymbol{\xi},\mathbf{x}) q_j^1(\boldsymbol{\xi},\mathbf{x}) + F_{ij}^2(\boldsymbol{\xi},\mathbf{x}) q_j^2(\boldsymbol{\xi},\mathbf{x}) + F_{ij}^3(\boldsymbol{\xi},\mathbf{x}) q_j^3(\boldsymbol{\xi},\mathbf{x}) \right] d\Gamma(\mathbf{x}). \tag{21}$$

It is important to notice that the distributed moment m_n may vary in its value and direction. In the above derivations, we pay no attention to the possibility of changes in the direction of the applied moment from one field point to another. Hence, the presented expressions are valid only to distributed forces in Cartesian directions.

4. ASSEMBLED PLATE STRUCTURES

Before the individual analysis of each laminate, a local coordinate system and the vectors composing its associated orthonormal basis $(\mathbf{e}'_1, \mathbf{e}'_2, \mathbf{e}'_3)$ must be defined, as illustrated in Fig. 5. These vectors must be decomposed in the directions of the global coordinate system, as follows

$$\mathbf{e}'_1 = {e'_1}^1 \mathbf{e}_1 + {e'_1}^2 \mathbf{e}_2 + {e'_1}^3 \mathbf{e}_3, \quad \mathbf{e}'_2 = {e'_2}^1 \mathbf{e}_1 + {e'_2}^2 \mathbf{e}_2 + {e'_2}^3 \mathbf{e}_3, \quad \mathbf{e}'_3 = {e'_3}^1 \mathbf{e}_1 + {e'_3}^2 \mathbf{e}_2 + {e'_3}^3 \mathbf{e}_3, \tag{22}$$

where $\mathbf{e}_i$ are the vectors of the orthornormal basis associated to the global coordinate system and ${e'}_i^j$ is the component of the vector $\mathbf{e}'_i$ in x_j direction.

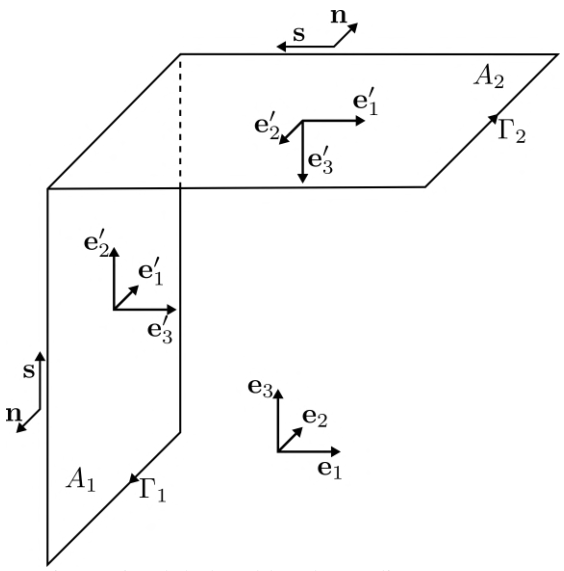

Figure 5: Global and local coordinate systems

The displacements at a node j can be transformed from global to local coordinates as follows

$$\begin{Bmatrix} u'_0 \\ v'_0 \\ w' \\ \beta'_n \end{Bmatrix}_j = \begin{bmatrix} {e'_1}^1 & {e'_1}^2 & {e'_1}^3 & 0 \\ {e'_2}^1 & {e'_2}^2 & {e'_2}^3 & 0 \\ {e'_3}^1 & {e'_3}^2 & {e'_3}^3 & 0 \\ 0 & 0 & 0 & 1 \end{bmatrix} \begin{Bmatrix} u_0 \\ v_0 \\ w \\ \beta_n \end{Bmatrix}_j \implies \mathbf{u}'_j = \mathbf{T}\mathbf{u}_j. \tag{23}$$

The same approach can be applied in order to transform surface tractions and transverse shear force, i.e.

$$\mathbf{t}'_j = \mathbf{T}\mathbf{t}_j. \tag{24}$$

Applying Eq. (8) for an arbitrary laminated plate discretized into M segments with N nodes, the following system of equations can be written

$$\sum_{j=1}^{N} \left\{ \widetilde{\mathbf{Y}}'_{ij} \mathbf{u}'_j - \mathbf{G}'_{ij} \mathbf{t}'_j \right\} = \mathbf{q}_i^*, \quad i = 1, 2, \ldots, N, \tag{25}$$

where $\widetilde{\mathbf{Y}}'_{ij}$ and $\mathbf{G}'_{ij}$ are the influence coefficients referred to the local system. Substituting Eq. (23) and Eq. (24) into Eq. (25), we get

$$\sum_{j=1}^{N}\left\{\widetilde{\mathbf{Y}}'_{ij}\mathbf{T}\mathbf{u}_j - \mathbf{G}'_{ij}\mathbf{T}\mathbf{t}_j\right\} = \mathbf{q}_i^*, \quad i = 1, 2, \ldots, N. \tag{26}$$

The equations above can be rearranged in the same form of Eq. (8) by introducing the following definitions

$$\hat{\mathbf{G}}_{ij} = \mathbf{G}'_{ij}\mathbf{T}, \quad \hat{\mathbf{Y}}_{ij} = \widetilde{\mathbf{Y}}'_{ij}\mathbf{T}, \tag{27}$$

leading to a system of equations whose variables are referred to global directions

$$\sum_{j=1}^{N}\left\{\hat{\mathbf{Y}}_{ij}\mathbf{u}_j - \hat{\mathbf{G}}_{ij}\mathbf{t}_j\right\} = \mathbf{q}_i^*, \quad i = 1, 2, \ldots, N. \tag{28}$$

Considering a set of N_l plates jointed together at the same edge and choosing one of them as the reference plate, e.g. plate 1, as discussed in Tanaka and Miyazaki (1985), the continuity conditions of displacements on the edge yield

$$u_0^i = u_0^1, \quad v_0^i = v_0^1, \quad w_0^i = w^1, \quad \beta_n^i = \gamma^i \beta_n^1, \quad i = 2, \ldots, N_l, \tag{29}$$

where the superscript i denotes the plate number and $\gamma^i = 1$ when the tangential direction of the jointed edge is the same as that of the reference plate, and otherwise $\gamma^i = -1$ (Fig. 6b). The equilibrium equations come from the condition that the resulting forces and moments on the jointed edge must be zero, that is

$$\sum_{i=1}^{N_l} T_x^i + T_x = 0, \quad \sum_{i=1}^{N_l} T_y^i + T_y = 0, \quad \sum_{i=1}^{N_l} V_n^i + V_n = 0, \quad M_n^1 + \sum_{i=2}^{N_l} \gamma^i M_n^i + M_n = 0, \quad i = 2, \ldots, N_l. \tag{30}$$

In the above, the terms without superscript represent the loads applied along the edge (Fig. 6a). Thus, for each interface node, either the forces and moments applied or the displacements must be prescribed.

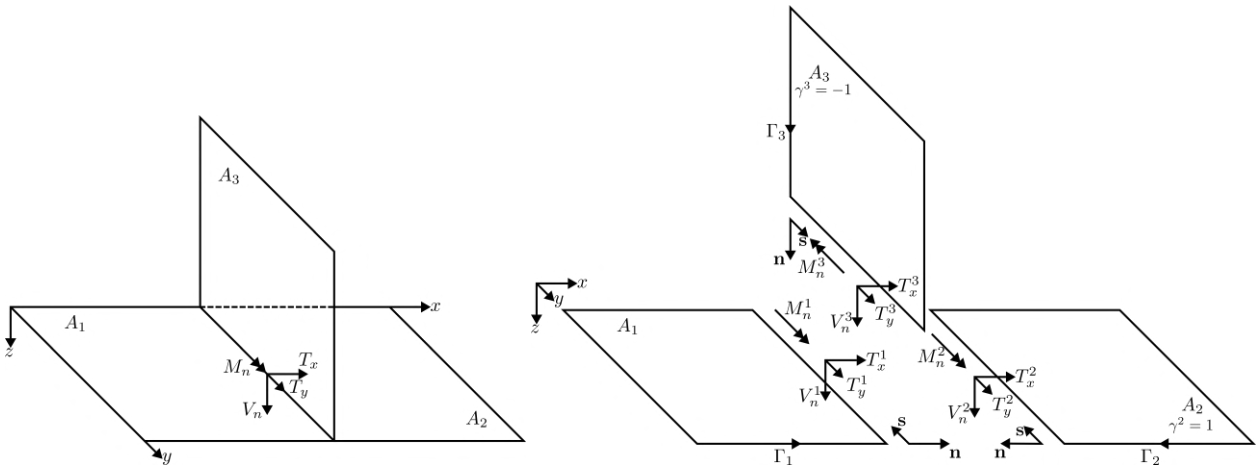

(a) Forces and moments applied along the interface edge (b) Resulting forces and moments for each plate in global coordinates

Figure 6: Assembled plate structure

5. NUMERICAL EXAMPLES

All the laminates studied in the following examples are made up by graphite-epoxy fiber-reinforced lamina whose material properties are $E_1 = 207$ GPa, $E_2 = 5.2$ GPa, $G_{12} = 3.1$ GPa, $\nu_{12} = 0.25$; and their laminae stacking sequence is $[0/45/90/0/-45/90/0/45/90]$.

5.1 Simply supported laminated plate under non-uniformly distributed transverse load

Before we discuss assembled plate structures, it is important to verify the validity and correctness of the boundary integral expressions for terms related distributed domain loads. To verify these expressions, a symply supported plate

with dimensions 1 m $\times$ 1 m $\times$ 10 mm and a square hole of side length 0.2 m in its center is considered (Fig. 7b). The laminated plate is assumed under a non-uniformly distributed transverse load described in local coordinates by:

$$q(x)(\text{kPa}) = 8.5x_1 - 1.5x_2 + 0.25 + x_1x_2. \tag{31}$$

The load distribution and the local coordinate system are shown in Fig. 7a.

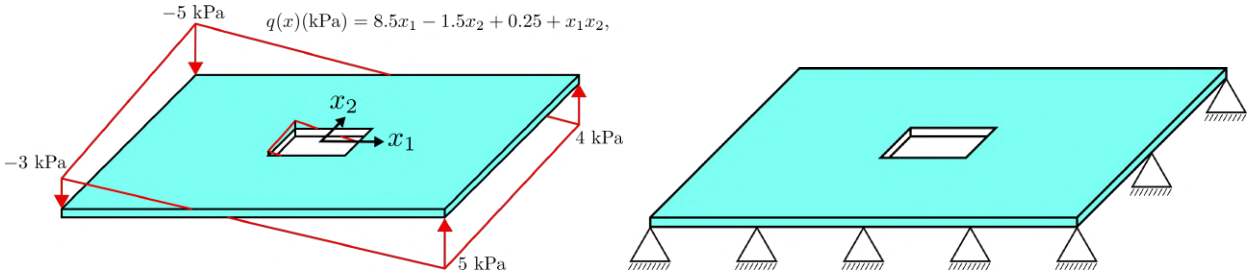

(a) Distributed load (b) Boundary conditions

Figure 7: Simply supported laminated plate under non-uniformly distributed transverse load

Each outer edge of the laminated plate was discretized into 20 boundary elements, and each inner edges into 10 elements, performing a total of 120 boundary elements. To compare the results, the structure was simulated using the commercial finite element software Abaqus, employing 19,840 triangular elements STRI3, which according to the Abaqus Theory Manual, impose the Kirchhoff constraint analytically and involves no transverse shear strain energy calculation.

The following table arranges the results for displacements and moments at some representative points. From this table, we can verify that the numerical results presented here are close to those provided by Abaqus, which verify the correctness of the boundary integral expressions derived in this paper. To show the effects of the distributed loads in the unsymmetric laminated plate, the deformed plate and the total displacement magnitude are represented in Fig. 8.

Table 1: Results for displacements and bending moments at representative points

Point		u_0	v_0	w	M_x	M_y	M_{xy}
(-400,0)	BEM	2.7165e-4	-1.9499e-4	-8.6786e-2	-4.3212e+1	-9.2311	-5.0029
	Abaqus	-2.7110e-4	-1.9529e-4	-8.6797e-2	-4.3215e+1	-9.2306	-5.0010
(-300,0)	BEM	-8.7649e-4	-3.5059e-4	-1.1251e-1	-5.3930e+1	-1.1862e+1	-7.2780
	Abaqus	-8.7456e-4	-3.5075e-4	-1.1255e-1	-5.3925e+1	-1.1832e+1	-7.2806
(-200,0)	BEM	-1.4534e-3	-4.5645e-4	-6.1541e-2	-3.7240e+1	-8.3219	-5.4205
	Abaqus	-1.4490e-3	-4.5570e-4	-6.1625e-2	-3.7112e+1	-8.3003	-5.4156

Unit: u_0, v_0 w (mm), M_x, M_y, M_{xy} (N mm/mm).

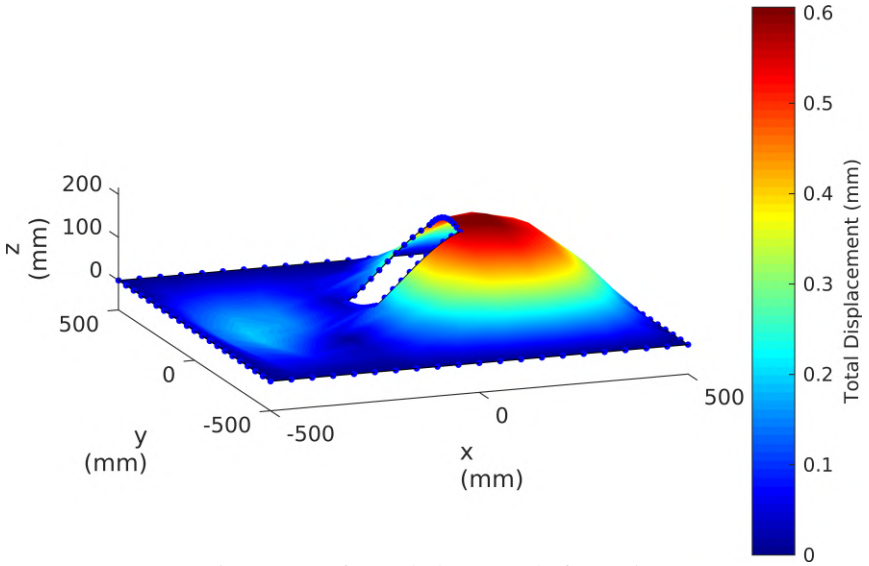

Figure 8: Deformed plate - Scale fator=500

5.2 T-shaped structure with a hole under non-uniformly distributed transverse load

In order to verify the boundary element formulation for assembled laminated plate structures, a T-shaped structure composed by three laminated square plates with the same dimensions of the previous example, one of them with a square hole of side length 0.2 m located in its center, is taken into consideration. One edge of the structure is clamped whereas all others are free, as shown in Fig. 9a. Non-uniform loads, transversal with respect to the surface region, are applied in the second and third laminates. Their distribution are described in local coordinates by

$$q(x)(\text{kPa}) = 0.2x_1(\text{m}) + 0.1, \text{ at the second plate}, \quad q(x)(\text{kPa}) = -0.2x_1(\text{m}) - 0.1, \text{ at the third plate}. \tag{32}$$

Each edge of the hole was discretized into 20 elements and all the other edges into 40 elements, resulting in a total of 560 boundary elements for the entire structure. In order to ensure accurate and efficient treatment for singular integrals, they were evaluated analytically using the solutions presented in Hwu and Chang (2015b). The structure was simulated using the software Abaqus, employing 94,512 triangular elements STRI3. The results for displacements in global directions x, y and z and bending moments in local directions x' and y', obtained at some representative points are arranged in Tab. 2. From this table we can verify that all results present a good agreement with those provided by Abaqus. The deformed structure and the total displacement magnitude $\left(\sqrt{u_0^2 + v_0^2 + w^2}\right)$ are represented in Fig. 9b. Finally, the bending moment $M_{x'}$ and the resultant force $N_{y'}$ along the structure are presented in Fig. 10.

Table 2: Results for displacements and bending moments at representative points

Point		u_0	v_0	w	$M_{x'}$	$M_{y'}$	$M_{x'y'}$
(0,500,500)	BEM	-1.5998	6.2007e-4	5.0341e-3	5.1921e+1	5.0921	3.9364
	Abaqus	-1.6006	6.1766e-4	5.0385e-3	5.1916e+1	5.0711	3.9016
(500,200,1000)	BEM	-4.7690	7.8483e-1	3.1918	-2.5602e+1	2.3236	-1.5427
	Abaqus	-4.7694	7.9043e-1	3.1949	-2.5613e+1	2.3253	-1.5532
(500,800,1000)	BEM	-5.7118	7.8542e-1	3.0212	-2.4026e+1	-1.0542	-2.3134
	Abaqus	-5.7188	7.9102e-1	3.0254	-2.3936e+1	-1.0983	-2.3114
(0,500,1500)	BEM	-1.0224e+1	6.0814e-4	9.7671e-3	2.0744e+1	1.2763	7.3109e-1
	Abaqus	-1.0231e+1	6.0714e-4	9.7754e-3	2.0767e+1	1.2658	7.2816e-1

Unit: u_0, v_0 w (mm), $M_{x'}$, $M_{y'}$, $M_{x'y'}$ (N mm/mm).

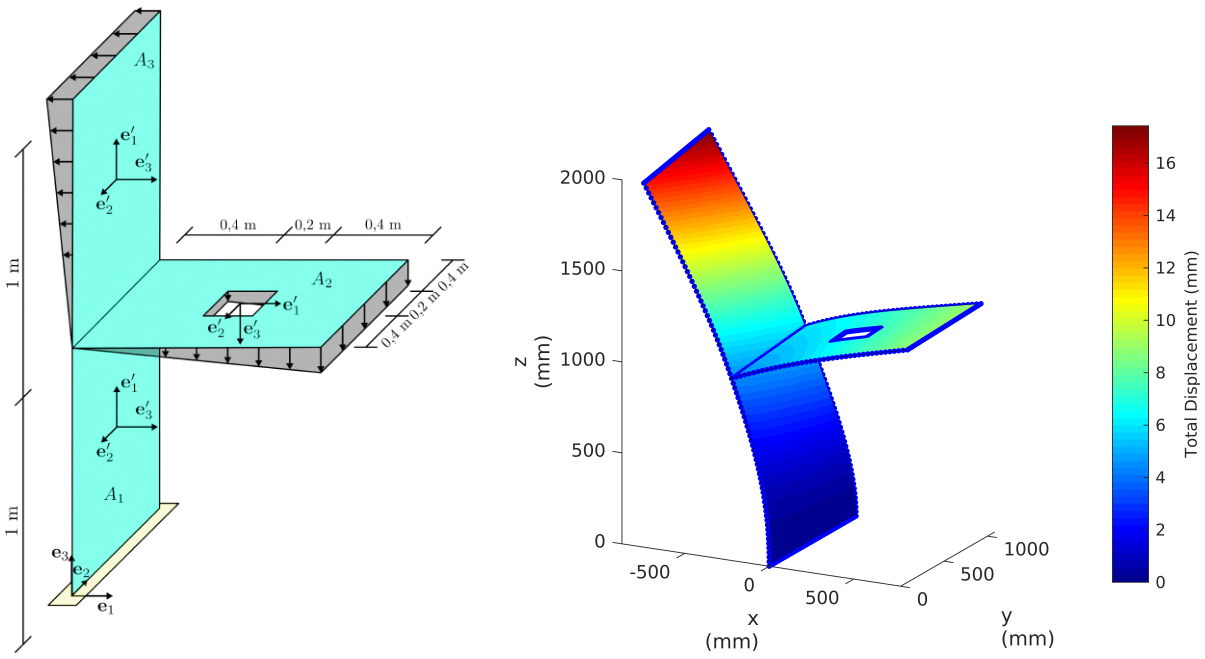

(a) Problem definition (b) Deformed structure - Scale factor = 50

Figure 9: T-shaped structure with a square hole under non-uniform transverse load

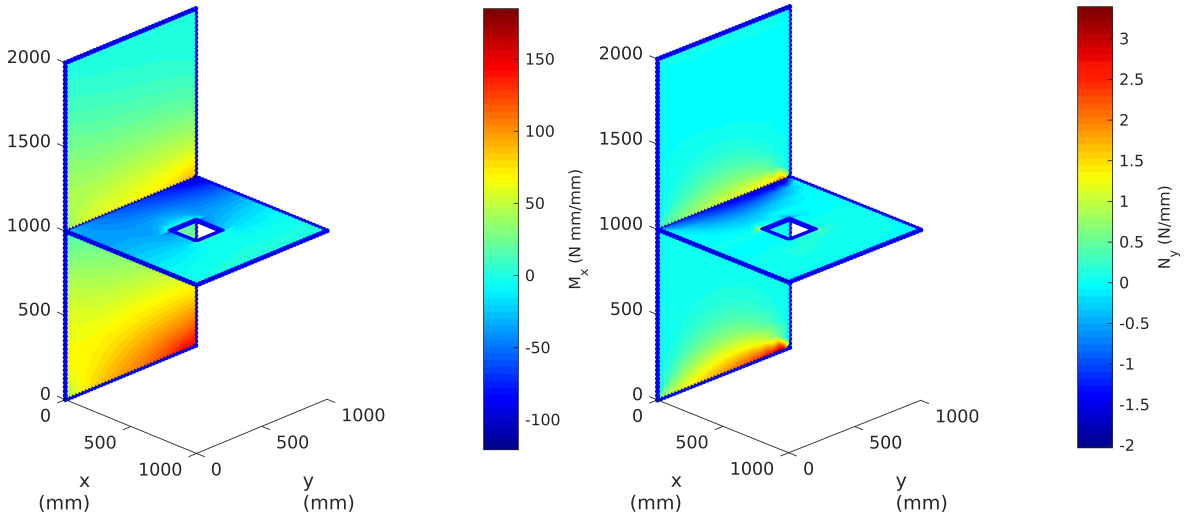

(a) $M_{x'}$ (b) $N_{y'}$

Figure 10: Stress resultant and bending moment along the structure.

6. CONCLUSIONS

We extended the boundary element formulation for the coupled stretching-bending analysis of thin laminated plates to three-dimensional assembled thin laminated plate structures. We also presented boundary integral expressions for terms related to non-uniformly distributed loads on the surface region of a laminated plate, avoiding the need to perform domain integrals, and improving the computational efficiency of the boundary element code. Since no singular integrals arise in these expressions, we can use standard Gaussian quadrature rule to evaluate them. The form assumed to the distributed loads is particularly interesting once we can use the resulting expressions to study distributed loads with uniform, linear and affine variation, and even bilinear interpolated loads. All the numerical results presented here are very close to those provided by the software Abaqus using very well refined finite element meshes, certifying the validity, reliability, and accuracy of the present formulation.

7. ACKNOWLEDGEMENTS

Caio C. R. Ramos was supported by grant #017/12205-7, São Paulo Research Foundation (FAPESP).

8. REFERENCES

Chang, H.W. and Hwu, C., 2016. "Complete solutions at or near the boundary nodes of boundary elements for coupled stretching-bending analysis". *Engineering Analysis with Boundary Elements*, Vol. 72, p. 89–99.

Gao, X.W., 2002. "The radial integration method for evaluation of domain integrals with boundary-only discretization". *Engineering Analysis with Boundary Elements*, Vol. 26, p. 905–916.

Hwu, C., 2003. "Stroh-like formalism for the coupled stretching–bending analysis of composite laminates". *International Journal of Solids and Structures*, Vol. 40, p. 3681–3705.

Hwu, C., 2010. "Boundary integral equations for general laminated plates with coupled stretching–bending deformation". *Proceedings of the Royal Society A*, Vol. 466, p. 1027–1054.

Hwu, C., 2012. "Boundary element formulation for the coupled stretching–bending analysis of thin laminated plates". *Composite Structures*, Vol. 36, No. 6, pp. 1027–1039.

Hwu, C. and Chang, H.W., 2015a. "Coupled stretching–bending analysis of laminated plates with corners via boundary elements". *Composite Structures*, Vol. 120, pp. 300–314.

Hwu, C. and Chang, H.W., 2015b. "Singular integrals in boundary elements for coupled stretching–bending analysis of unsymmetric laminates". *Composite Structures*, Vol. 132, pp. 933–943.

Palermo Junior, L., 1989. *Análise de peças de seção delgada como associação de placas pelo método dos elementos de contorno*. Ph.D. thesis, Universidade de São Paulo, São Carlos, Brasil.

Tanaka, M. and Miyazaki, K., 1985. "A direct BEM for elastic plate-structures subjected to arbitrary loadings". In *Boundary elements VII*. Brebbia, C. A. and Maier, G. (eds.), Springer-Verlag, Berlin, p. 4/3–4/16.

9. RESPONSIBILITY NOTICE

The authors are the only responsible for the printed material included in this paper.